

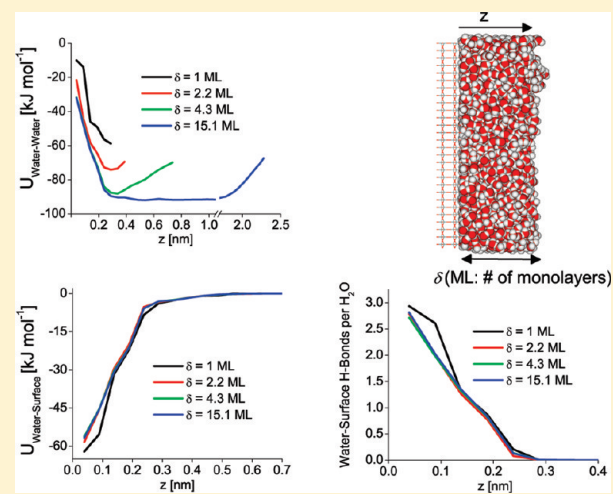
Structure and Energetics of Thin Film Water

Santiago Romero-Vargas Castrillón,[†] Nicolás Giovambattista,[‡] Ilhan A. Aksay,[†] and Pablo G. Debenedetti^{*,†}

[†]Department of Chemical and Biological Engineering, Princeton University, Princeton, New Jersey 08544-5263, United States

[‡]Physics Department, Brooklyn College of the City University of New York, Brooklyn, New York 11210, United States

ABSTRACT: We present a molecular dynamics (MD) simulation study of the structure and energetics of thin films of water adsorbed on solid substrates at 240 K. By considering crystalline silica as a model hydrophilic surface, we systematically investigate the effect of film thickness on the hydrogen bonding, density, molecular orientation, and energy of adsorbed water films over a broad surface coverage range (δ). At the lowest coverage investigated ($\delta = 1$ monolayer, ML), >90% of water molecules form three hydrogen bonds (H-bonds) with surface silanol groups and none with other water molecules; when $\delta = 1$ ML, the most probable molecular orientation is characterized by both the molecular dipole and the OH vectors being parallel to the surface. As δ increases, water–water and water–surface interactions compete, leading to the appearance of an orientational structure near the solid–liquid interface characterized by the dipole moment pointing toward the silica surface. We find that the water–surface H-bond connectivity and energetics of the molecular layer nearest to the solid–liquid interface do not change as δ increases. Interfacial water molecules, therefore, are able to reorient and form water–water H-bonds without compromising water–surface interactions. The surface-induced modifications to the orientational structure of the adsorbed film propagate up to ~ 1.4 nm from the solid–liquid interface when $\delta = 15.1$ ML (a film that is ~ 2.3 nm thick). For the thinner adsorbed films ($\delta \leq 4.3$ ML, thickness ≤ 0.8 nm) orientational correlations imposed by the solid–liquid and liquid–vapor interfaces are observed throughout.



1. INTRODUCTION

When a solid is exposed to ambient air, water molecules will adsorb on its surface forming a thin film a few molecular diameters in thickness. Understanding the properties of adsorbed water films is of relevance to many scientific fields—from climatology to catalysis—given that water's molecular structure determines many of the physical and chemical properties of the interface and underlying material,^{1,2} such as its chemical reactivity, corrosion, and the transport of coadsorbed molecules. In addition, wetting phenomena can only be comprehended inasmuch as the properties of adsorbed water are known. This is due to the fact that molecular-scale water films are the structural precursors of (macroscopic) multilayer films.³ Indeed, it can be speculated that the different values of the contact angle of water on hydrophilic surfaces (e.g., silica vs titania) result from the subtle interplay between the molecular structure of water in a droplet and that of water molecules adsorbed on different substrates.

Despite the widespread occurrence and importance of thin water films, knowledge of the structure and properties of adsorbed water is still incomplete. While it is well understood that water's peculiar thermodynamic properties stem from its ability to form strong hydrogen bonds (H-bonds), the way in which the H-bond network is modified in the proximity of a

surface is not. This is the case even for widely studied “simple” systems, such as water adsorption on metal surfaces,^{4,1} where the existence of a hexagonal icelike bilayer, once considered paradigmatic, has been recently called into question.³ The picture is further complicated when the adsorbent is an oxide. In this case, water molecules can form H-bonds with surface hydroxyl groups, whose strength is comparable to a water–water H-bond (~ 15 – 25 kJ mol⁻¹). In light of this, one is led to ask whether the structure of adsorbed water is dictated by surface–water interactions or by water–water H-bonds.⁵ The latter raises a further question: how is the interfacial structure modified by water–water interactions when multiple layers are adsorbed? After adsorption of a few water layers, thermal fluctuations are likely to blur the effect of the solid surface on the local density, molecular orientation and H-bond connectivity, leading to random, bulklike structural properties. A precise knowledge of the range of surface-induced perturbations is necessary.

In this paper, we explore the questions raised above through molecular dynamics (MD) simulations of thin water films adsorbed on hydrophilic silica, an oxide which, in addition to

Received: September 2, 2010

Revised: January 18, 2011

Published: February 25, 2011

being the major component of the Earth's crust, finds a myriad applications in electronics, agriculture, metallurgy, and biochemistry.⁶ Water films adsorbed on silica have been studied by various computational techniques (density functional theory, ab initio, and classical MD^{7–10}) and different experimental techniques, such as attenuated total reflection infrared spectroscopy (ATR-IR),^{11,12} atomic force and Kelvin probe microscopy,^{5,13} and sum-frequency vibrational spectroscopy.^{14,15} These studies have uncovered the rich phenomenology of interfacial systems, showing that water undergoes extensive modifications to its H-bond network in proximity of the silica surface, often forming ordered, icelike structures.^{9,11} However, most computational studies have not explored the structure of films beyond one adsorbed layer, and their interpretation remains contentious¹⁶ due to system size constraints and the short time scales accessible to simulations, particularly when ab initio methods are used. These limitations notwithstanding, molecular simulations remain a valuable tool in surface science, often complementing and aiding the interpretation of experimental data. Provided accurate intermolecular potentials are available, molecular simulations provide a level of microscopic detail, such as the determination of the orientational structure at an interface, that is difficult to attain with state-of-the-art experimental techniques.

In this simulation study, our objective is to explore the modifications undergone by the structure of water in the vicinity of a hydrophilic silica surface. We focus on the variation of local H-bonding, molecular orientation, density, and adsorption energy, with the number of adsorbed layers (δ). In addition to providing insight into the relative influence of water–water, versus water–surface interactions, this study allows us to evaluate the range of surface-induced perturbations. The above objectives are realized by varying δ from 1 monolayer (ML) to \sim 15 adlayers. We find that the structure of a 1 ML film is significantly different to that of thicker, multilayer films, its H-bonding network and orientational order being determined by surface water interactions. Increasing the number of adsorbed layers results in water–water interactions becoming equally relevant in determining the structure of the adsorbed film.

2. SIMULATION AND COMPUTATIONAL DETAILS

We perform molecular dynamics simulations in the canonical (constant N,V,T) ensemble at a temperature of 240 K,⁴⁹ controlled by means of a Berendsen thermostat.¹⁷ The SPC/E pair potential, a rigid, three-site model,¹⁸ is used to compute water–water interactions. Simulations were carried out in a cubic box of side length $L = 6.93$ nm, into which we introduce a hydroxylated silica surface (dimensions $L \times L \times 0.866$ nm) parallel to the x,y -plane, such that the plane containing the surface H atoms lies at $z = -2.5$ nm. Periodic boundary conditions are applied in the x and y directions, making the system macroscopic in the directions parallel to the surface; a reflective boundary condition is applied at $z = 3.0$ nm, imposing a small vapor pressure on the system. We consider an atomically detailed surface representation of the (111) plane of β -cristobalite, a crystalline phase of silica. The surface is hydroxylated with 224 OH groups, resulting in a hydroxyl group surface density of 4.66 OH nm^{-2} , in good agreement with the experimental value of 4.55 OH nm^{-2} for the (111) plane of cristobalite.⁶ Water–surface interactions are computed with the potential proposed by Lee and Rossky,¹⁹ which allows for Lennard-Jones interactions between the water

oxygen and surface Si and O atoms, and Coulombic interactions between the water atoms and surface silanol (SiOH) groups. All Si and O surface atoms remain fixed during the simulation; surface H atoms can reorient in a circular trajectory with a fixed bond length of 0.1 nm and fixed Si–O–H angle of 109.47° . Long-range electrostatics are handled with the Ewald sum method,²⁰ using a real-space cutoff of 0.79 nm, $k_{\max} = 5^3$ reciprocal space vectors and a screening-charge Gaussian distribution with $\alpha = 4.0 \text{ nm}^{-1}$.

Experiments and ab initio simulations^{21,15,22} have shown that surface silanol groups exhibit bimodal acidity manifested by pK_a values at ~ 4.5 and ~ 8.5 , the latter value characterizing the majority of the surface groups (the higher acidity seems to emerge only in strained and sparsely hydroxylated regions of the surface²²). Accounting for these effects requires the use of dissociative potentials or ab initio techniques.^{22–24} However, assuming neutral pH and $pK_a = 8.5$, the ratio SiOH:SiO[−] is estimated at ~ 32 , implying that only ca. 3% of surface silanol groups would exist in the ionized state. Therefore, use of a nondissociative potential appears to be justified under the assumed conditions given the small number of SiO[−] groups. Nonetheless, future work should focus on systems for which the aforementioned assumptions are invalid, such as non-neutral pH or defective surfaces, both of which require the use of ab initio or dissociative potentials.

Molecular simulations of adsorbed systems are commonly performed in the grand canonical ensemble using the Monte Carlo (MC) method,^{25–27} or with hybrid algorithms combining short MD runs with MC particle insertion/removal steps,^{28,29} that also allow examination of the adsorption dynamics. In both methods, the adsorbent and adsorbate are in equilibrium with a reservoir at constant chemical potential (μ) and T ; consequently, the particle number fluctuates about $\langle N \rangle$ and a solid–liquid–vapor interfacial system is established allowing the calculation of the adsorption isotherm. Our simulations, on the other hand, were performed for a fixed N , the choice being guided by the class of properties to be calculated. In our study we perform independent simulations at different N and systematically vary the number the adsorbed layers; i.e., we examine the effect of δ on adsorbed film structural properties. Precise knowledge of the chemical potential (or partial pressure) that results in a particular value of δ is beyond the scope and objectives of our study. Therefore, equilibration in the grand canonical ensemble is not necessary.

We study thin films of water with δ ranging from 1 to \sim 15 ML. The definition of monolayer (ML) adopted here is based on the morphology of the silica surface, which contains 224 hydroxyl groups that can act as potential adsorption sites. Accordingly, δ is defined as the ratio of water molecules to surface hydroxyl groups. We explored values of δ ranging from 1 to 15.1 ML; to this end, we investigated systems with 224 ($\delta = 1$ ML), 486 ($\delta = 2.2$ ML), 961 ($\delta = 4.3$), and 3375 ($\delta = 15.1$ ML) SPC/E water molecules. The initial configuration of water in films with $\delta \leq 4.3$ ML was obtained from a MD simulation of water confined by two hydrophilic silica surfaces, identical to those used in this work, placed 5.0 nm apart. After equilibration in the NVT ensemble for 500 ps at 300 K and a mean density of 1 g cm^{-3} , we selected molecules within slabs of dimensions $L \times L \times i$ nm (where $i = 0.13, 0.3, \text{ and } 0.6$ nm for $\delta = 1, 2.2, \text{ and } 4.3$ ML, respectively), located near the center of the confined volume. All selected molecules were at a distance ≥ 2.2 nm from the nearest silica surface and showed bulklike structural and dynamic properties.³⁰

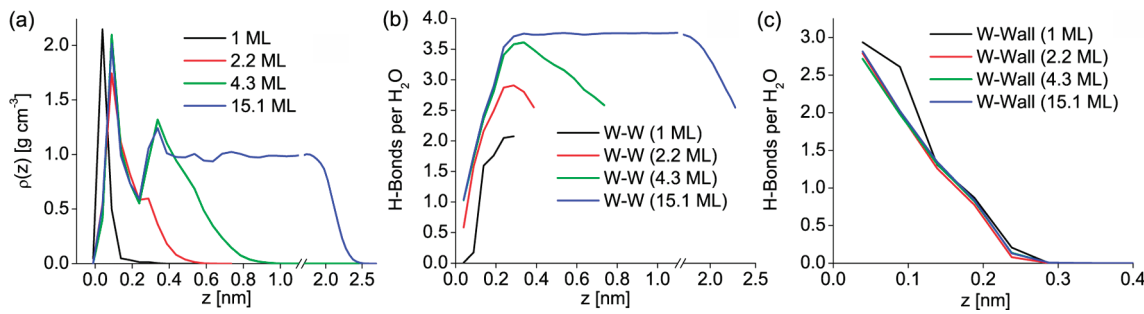


Figure 1. (a) Local density profile, $\rho(z)$, computed in 0.05 nm thick slabs, as a function of the distance from the solid–liquid interface, z (the surface H atoms are located at $z = 0$). (b) Number of water–water (W–W) H-bonds per molecule as a function of z . (c) Same as (b), for water–surface (W–Wall) H-bonds.

To finalize the initial configuration of the adsorbed film, the molecules thus selected were translated in the z direction toward the silica surface, leaving a gap of 0.2 nm (i.e., ca. one water molecular diameter) between the surface H atoms and the lower edge of the water slab. To prepare the 15.1 ML system, a cubic configuration of bulk water (side length = 4.66 nm, density 1 g cm^{-3}) was placed near the silica surface, leaving a gap of 0.2 nm between the surface H atoms and the side of the water cube closest to the surface. After equilibration at 300 K for 1.0 ns the water had wetted the surface entirely, forming a film with dimensions $L \times L \times \sim 2.3 \text{ nm}^3$. The resulting configuration was used as input for the 15.1 ML system.

All simulations involved an equilibration time of 1.0 ns followed by a production time of 1.5 ns when $\delta = 15.1 \text{ ML}$ and 3.0 ns for $\delta \leq 4.3 \text{ ML}$. Our simulations appear to be sufficiently long (at least $\sim 140\tau$, where $\tau = 17 \text{ ps}$ is the structural relaxation time of bulk SPC/E water at 240 K and 1 g cm^{-3})³¹ to avoid metastable artifacts. The equations of motion were integrated using the leapfrog scheme³² with a time step of 1.0 fs. Water molecular geometry was constrained using the SHAKE algorithm.³³ Further details on the simulation may be found elsewhere.^{34,35}

3. RESULTS AND DISCUSSION

In this section we characterize the structure and energetics of thin water films as a function of distance from the interface, z , and number of adsorbed water layers, δ . For all results presented below, the solid–liquid (sl) interface, defined as the plane containing the surface hydrogen atoms, is located at $z = 0$. Results reflect averages over 501 configurations saved every 1 ps.

3.1. Local Structure: Density and H-Bond Connectivity. Figure 1a presents the density profile (i.e., the variation of local density with distance from the sl interface, z), computed in 0.05 nm thick slabs parallel to the surface. The position of the water O atoms was used to construct the $\rho(z)$ profile. The system with $\delta = 1 \text{ ML}$ shows a single, high-density peak at $z = 0.039 \text{ nm}$ from the interface, while the oscillations in $\rho(z)$ characteristic of a liquid near a hard surface are observed in thicker films. We note that the first peak in the density profile ($z < 0.2 \text{ nm}$) moves farther from the interface when $\delta \geq 2.2 \text{ ML}$, in which case it is found at $z = 0.089 \text{ nm}$. This shift is attributed to water–water H-bonds prevalent when $\delta > 1 \text{ ML}$ (vide infra). A second peak is apparent in the systems with 4.3 and 15.1 ML, at $z = 0.338 \text{ nm}$. At $z \approx 1 \text{ nm}$ the density of the 15.1 ML system converges to a constant bulk density of 1 g cm^{-3} ($P = 0 \text{ GPa}$, $T = 240 \text{ K}$).

Panels b and c of Figure 1 show the water–water (W–W) and water–surface (W–Wall) H-bond profiles for all the films.

In computing the number of H-bonds per molecule, we adopted a geometric definition according to which two species are H-bonded if the distance between the O atoms is less than 0.36 nm (roughly the range of the first coordination shell of bulk water, and of water under hydrophilic confinement as determined from the surface oxygen–water oxygen radial distribution function^{35,36}) and the O–H \cdots O angle is less than 30° . The latter angular cutoff value is obtained from the amplitude of the librations that break H-bonds, which have been determined to be $\sim 30^\circ$.³⁷

A different H-bond network connectivity appears as δ increases. In Figure 1b we first note that the number of W–W H-bonds at $\delta = 1 \text{ ML}$ is ~ 0 at $z = 0.039 \text{ nm}$, the distance at which the density profile exhibits the only peak for this film, while the number of W–Wall H-bonds is 3, as shown in Figure 1c. At slightly larger distances ($z \approx 0.2 \text{ nm}$), the number of W–W H-bonds increases to ~ 2 ; these H-bonds, however, involve less than 5% of all water molecules in the monolayer. Thus the 1 ML film is comprised of molecules which mainly H-bond to surface silanol groups. A similar adsorbed water structure was observed in density functional theory (DFT) calculations of water adsorption on the β -cristobalite (111) surface.⁸

The number of W–W H-bonds per molecule is seen to rise quickly upon increasing the number of adlayers. As δ increases to 2 or more layers there is a net gain between 1 and 2 W–W H-bonds at $z = 0.089 \text{ nm}$ (cf. the increase in W–W H-bonds to ~ 1.7 in Figure 1b, for $\delta \geq 2.2 \text{ ML}$), coinciding with the first maximum of $\rho(z)$. An increase in film thickness from 2.2 to 4.3 ML, manifested by the appearance of the second maximum in $\rho(z)$, also results in a gain of ~ 1 W–W H-bond at $z = 0.338 \text{ nm}$. Figure 1b shows that when $\delta = 15.1 \text{ ML}$, water exhibits bulklike H-bonding when $0.4 \text{ nm} < z < 1.6 \text{ nm}$. At the liquid–vapor interface (lv), W–W H-bonding decreases, consistent with the decrease in water density. The W–W H-bond profiles (for $\delta > 1 \text{ ML}$) in Figure 1b were truncated at distances where the number of H-bonds per molecule is ~ 2.5 (at this distance the number of water molecules is ~ 10), i.e., a loss of 1 H-bond relative to bulk water. The loss of 1 H-bond per molecule near lv (and other hydrophobic) interfaces has been observed experimentally using sum-frequency generation (SFG) vibrational spectroscopy, which shows the abundance of free OH groups at this and other hydrophobic interfaces.³⁸ We have indeed found that, at the lv interface, there is, on average, one non-H-bonded OH group per molecule.

Figure 1c depicts the variation of the number of W–Wall H-bonds with z . We note that close to the silica surface ($z = 0$), all films form ~ 3 H-bonds with silanol groups. More importantly,

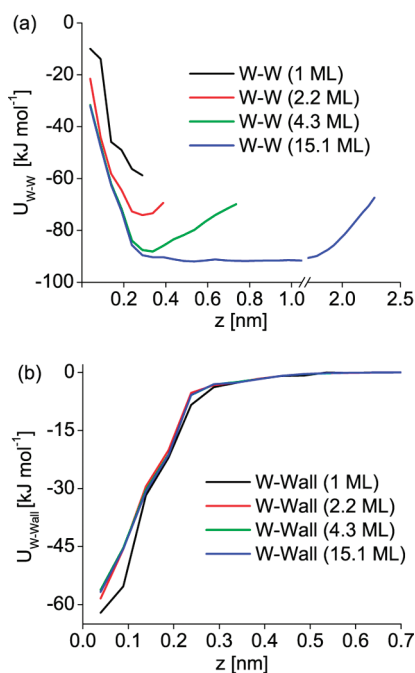


Figure 2. (a) Water–water local potential energy (U_{W-W}), computed in 0.05 nm thick slabs, as a function of distance from the interface, z . (b) Same as (a), for water–surface interactions (U_{W-Wall}).

the variation of the number of W–Wall H-bonds with z is nearly independent of the number of adsorbed layers, changing only slightly when δ increases from 1 to 2.2. This seemingly contradictory observation—that W–W H-bonding changes significantly while W–Wall does not—is explained by the fact that water near the sl interface reorients in order to form H-bonds with other molecules without compromising H-bonds with the surface. We will return to this observation in section 3.2.

We conclude this section with a discussion of the thin film energetics. Figure 2 presents the local potential energy profile, decomposed into its W–W and W–Wall contributions (U_{W-W} and U_{W-Wall} , respectively). The profiles in Figure 2 were computed in 0.05 nm thick slabs, in analogy to the density and H-bond calculations. We excluded the reciprocal component in the calculation of W–W and W–Wall electrostatic interactions, since this component amounts to <1% of the total potential energy of the system. The potential energy profiles are unaffected by this exclusion.

For all films, U_{W-W} becomes weaker (less negative) near the surface since this region is dominated by W–Wall H-bonds (note the strengthening of U_{W-Wall} when $z < 0.3$ nm in Figure 2b). Similarly W–W interactions are weakened by the lv interface. The 15.1 ML film exhibits a region ($0.5 \text{ nm} < z < 1.7 \text{ nm}$) where the W–W interaction energy remains constant at $\sim -92 \text{ kJ mol}^{-1}$. Division of the latter energy by the (bulklike) number of H-bonds per molecule observed over the same range of z , ~ 3.8 per water (cf. Figure 1b), results in an estimate of the H-bond energy of $\sim -24 \text{ kJ mol}^{-1}$. This number agrees with experimental values for the strength of the H-bond in ice and water, generally estimated at -15 to -25 kJ mol^{-1} .⁵⁰ In a similar fashion the strength of a W–Wall H-bond is estimated at $\sim -20 \text{ kJ mol}^{-1}$ based on the number of H-bonds and interaction energy at $z = 0$ in Figures 1c and 2b.⁵¹ For the systems under study, therefore, W–W interactions are slightly stronger than W–Wall H-bonds. Finally, we point out that the local W–Wall

interaction energy shown in Figure 2b is approximately independent of the film thickness, as one would expect in light of the surface H-bonding results in Figure 1c, which are also independent of δ .

3.2. Orientational Structure: Angular Distributions. We continue the structural analysis quantifying the orientational order in the adsorbed films. Our objective is to (a) characterize the local orientational structure near the sl interface, (b) describe the variation of the local orientational structure with film thickness, and (c) assess the distance from the interface within which the molecular orientation of water is influenced by the presence of the sl and lv interfaces.

To characterize the orientational order in the film, we use the following probability density function (pdf)³⁹

$$P_\mu(z, \theta) = \frac{\langle \delta(\theta - \theta') \rangle}{\sin \theta} \quad (1)$$

where the angle brackets denote an average over all angular measurements in a slab at a distance z from the interface (vide infra) and over 501 MD configurations; division by $\sin \theta$ removes the bias due to variations in the solid angle. In eq 1, θ' is the angle formed by the unit molecular dipole vector μ and the unit vector normal to the surface, pointing *into* the water film. We also use a pdf analogous to eq 1 to describe the orientational structure of water in terms of the angle between the unit normal and each of the vectors OH pointing from the water oxygen to each of the protons.

The probability density function in eq 1 is computed locally in 0.05 nm thick slabs parallel to the SiO_2 substrate, placed at various distances from the plane containing the surface hydrogen atoms (located at $z = 0$). Since eq 1 is undefined wherever the number of water molecules vanishes, we assigned to it a value of zero in regions without molecules (i.e., at the wall or beyond the lv interface).

Figures 3 and 4 present 3-D surface plots describing the spatial variation $P(\theta_{\mu}, z)$ and $P(\theta_{OH}, z)$ in films with a surface coverage ranging from $\delta = 1$ to 15.1 ML. Near the sl interface (located at $z = 0$), all panels in Figures 3 and 4 exhibit peaks in the pdf; the absence of flat regions (i.e., those where all molecular angles would have equal probability) near the sl interface shows the large degree of orientational order imposed by the solid surface. A similar observation can be made regarding the lv interface, whose location depends on the value of δ (vide infra). The influence of the sl and lv interfaces on water orientation is particularly clear in the films with $\delta = 1, 2.2$, and 4.3 ML, which show regions throughout the film where water molecules adopt preferential values of θ_{μ} and θ_{OH} .

Both experiments^{14,12,15,11,13} and simulations^{39,19,40} have studied the orientational order of water near sl interfaces. A number of these investigations^{13,11,12} have focused on assessing the distance from the sl interface at which the structure of water within a film adopts the randomness associated with the bulk state. Our study of the orientational structure allows us to assess this distance. Figures 3a–c and 4a–c demonstrate that films up to ~ 1 nm in thickness ($\delta \leq 4.3$ ML) do not exhibit regions of bulklike orientational structure, as the angular pdf's do not become flat for a finite range of z . Conversely, at a coverage of 15.1 ML (Figures 3d and 4d), we note that orientational correlations extend up to ~ 1.4 nm from the interface. Beyond this point, we find a region that is roughly within $1.4 \text{ nm} < z < 1.6$ nm showing a bulklike orientational structure. Within this

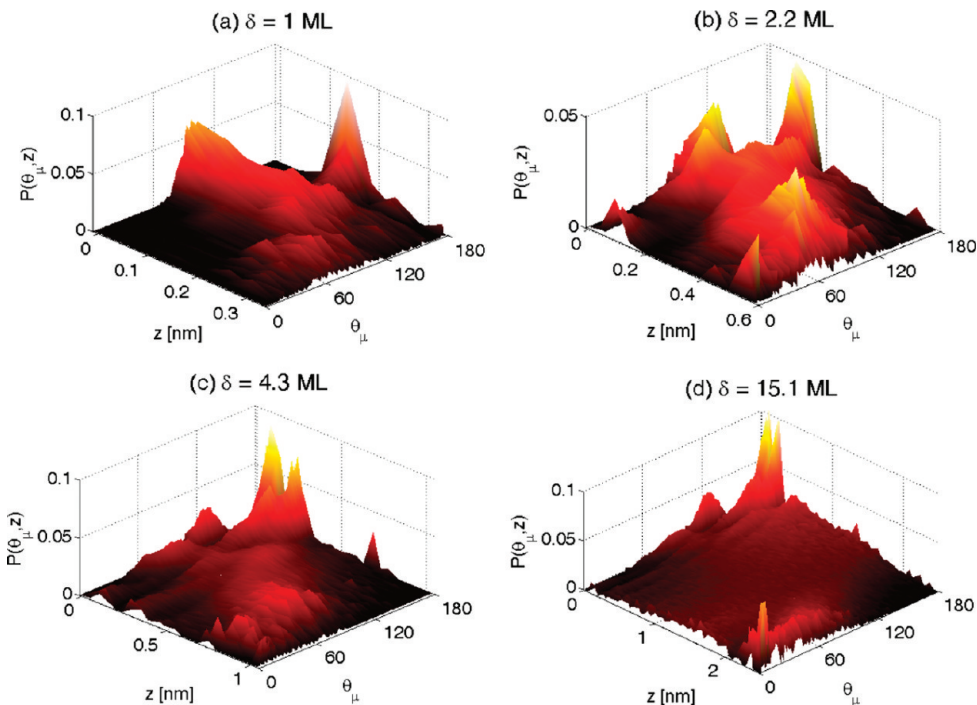


Figure 3. Variation of $P(\theta_{\mu}, z)$ (probability density function of water angular orientation) in thin water films denoted by their thickness (δ , number of adsorbed layers). The surface color code is proportional to peak height.

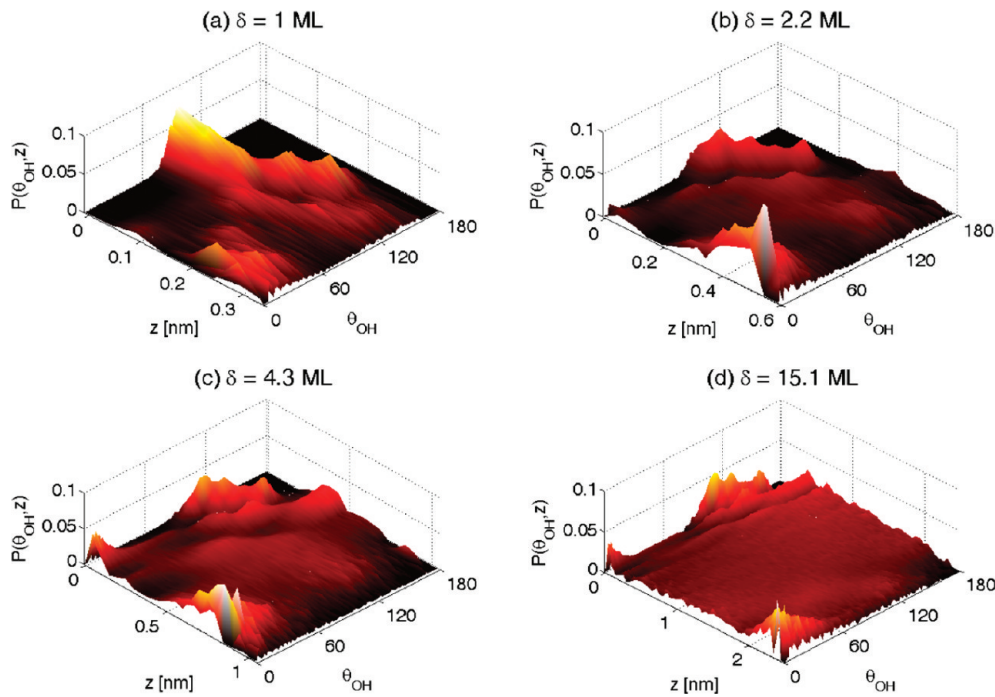


Figure 4. Variation of $P(\theta_{OH}, z)$ (probability density function of water angular orientation) in thin water films denoted by their thickness (δ , number of adsorbed layers). The surface color code is proportional to peak height.

slab of liquid, roughly one water molecular diameter thickness, both the θ_{μ} and θ_{OH} pdf's show weak or no orientational correlations (i.e., their respective pdf's are approximately flat). At $z > 1.6$ nm, the features characteristic of water orientation at a liquid/vapor interface, to be discussed below, become noticeable.

In a recent study of water adsorbed on hydrophilic silica, Verdaguer et al.¹³ report surface potential measurements that

reflect the preferential orientation of $\vec{\mu}$, proposing that 4–5 ML (or a film thickness of ~ 1.5 nm since, in their study, 1 ML ≈ 0.3 nm, water's van der Waals diameter), are sufficient for water to reach a bulklike structure. Similarly, Asay and Kim¹¹ and Barnette et al.,¹² based on their IR spectroscopy studies, proposed that the first four water layers show the largest substrate-induced perturbation, resulting in an "icelike" water structure at

the interface, and that the average molecular orientation becomes random when the adsorbed film thickness is $>1-1.5$ nm. Therefore, our simulation results are consistent with the experiments of refs 11–13 insofar as the solid-surface-influenced orientational structure is manifested within ~ 1.4 nm from the sl interface. It is important to indicate that the region of bulklike water orientation observed when $\delta = 15.1$ ML involves only $\sim 12\%$ of the molecules in the film; thus, the majority of the molecules, even at this value of δ , exhibit an orientation that is imposed by either the sl or the lv interface. The strong influence of the interfaces on the orientational structure contrasts with the local H-bonding connectivity and density; while the latter properties exhibit bulklike values over, e.g., $0.8 \text{ nm} < z < 1.4 \text{ nm}$, the orientational structure within this region is not flat. The stronger influence of the interfaces on orientational structure, relative to other structural properties, was also observed in MD simulations of SPC water on mica;⁴⁰ this study showed that even for the thickest film investigated (~ 3 nm) all molecules show evidence of orientational correlations.

Concerning water orientation at the lv interface, we note that near this interface (found at $z_{lv} \approx 0.3, 0.5, 0.8$, and 2.3 nm for $\delta = 1, 2.2, 4.3$, and 15.1 ML, respectively) water molecules lose one H-bond by pointing an OH vector into the vapor phase (hence the maximum in $P(\theta_{OH})$ at z_{lv} , found at $\sim 0^\circ$ and a smaller, broader peak at $\sim 120^\circ$; and a maximum in $P(\theta_\mu)$ at $\sim 60^\circ$). This orientational structure is characteristic of hydrophobic surfaces (of which the lv interface is an example) and has been previously observed in MD simulations of the water–vapor interface,^{41,42,55} of water near solid hydrophobic surfaces,³⁹ as well as in SFG vibrational spectroscopy experiments³⁸ and surface potential measurements.¹³ Also, for systems with $\delta > 1$ ML, Figure 3 shows that molecules in the outermost region of the lv interface orient their dipole vector in the direction parallel to the surface normal (hence the peak at $\theta_\mu \approx 0^\circ$ at the far edge of the lv interface that is most apparent in the 2.2 and 15.1 ML systems). Molecules with this orientation represent $<0.5\%$ of the molecules in the system.

So far the discussion has focused on the range of surface-influenced orientational structures. Additionally, it is important to observe that the orientational structure undergoes significant modifications as δ increases. For example, the single preferential orientation observed at 1 ML coverage (note the single peak centered at $90-100^\circ$ in Figures 3a and 4a, $z \approx 0$) evolves into multiple peaks as δ increases. In the following paragraphs we will characterize the dependence of the local orientational structure on δ ; in doing so, we will make connections with the local density and H-bonding information presented in section 3.1. We consider the system with $\delta = 1$ ML as starting point.

3.2.1. $\delta = 1$ ML. At a coverage $\delta = 1$ ML, molecules exhibit a single orientational structure, denoted by the single peak at $z = 0.039$ nm in Figures 3a and 4a ($z = 0.039$ nm is the location of the peak in $\rho(z)$ for 1-ML coverage; cf. Figure 1a). In Figure 5 we plot the θ_μ and θ_{OH} pdfs at $z = 0.039$ nm; the location of the peaks (at $\theta_\mu \approx 105^\circ$ and $\theta_{OH} \approx 99^\circ$) indicates that molecules are oriented parallel to the surface. To fully specify the structure, we must incorporate H-bond network information. As mentioned previously, molecules at $z = 0.039$ nm from the silica surface form 3 H-bonds with surface silanol groups and ~ 0 with other waters (cf. Figure 1b,c). Therefore, the inset to Figure 5 depicts the predominant water structure when $\delta = 1$ ML, characterized by 3-fold H-bonding with silanol groups (in which water donates two H-bonds to two vicinal surface O atoms and accepts a

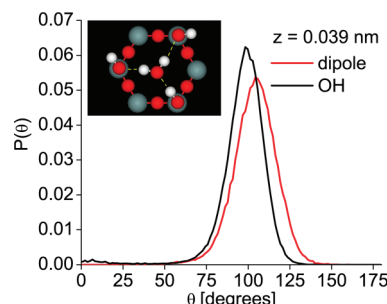


Figure 5. $P(\theta)$ probability density function describing the orientation of water in the 1 ML thin film (at $z = 0.039$ nm). The inset depicts the predominant molecular structure of water at 1 ML coverage (red spheres, O atoms; white, H atoms; gray, Si atoms), where one water molecule is found at the center of a hexagon formed by surface atoms. Water atoms are approximately coplanar to surface H atoms. The dashed yellow lines denote surface silanol–water H-bonds.

H-bond from a surface hydroxyl). This structure is in agreement with DFT calculations of the water– β -cristobalite system at 1 ML coverage.^{8,52} Moreover, it is consistent with experimental results of water adsorption on hydrophilic SiO_2 ¹³ which suggest that, in the early stages of adsorption (<2 ML), the dipole moment is either randomly oriented or pointing in a direction parallel to the interface.

The quasi-two-dimensional structure described above is characterized by water molecules which predominantly form H-bonds with surface silanol groups and only rarely with other water molecules. We will henceforth denote as “nonwetting” (NW) those molecules which form H-bonds with surface O and H atoms but not with other water molecules. Analysis of the final 1 ns of the simulation showed that the majority of molecules (ca. 93%) in the 1 ML system are NW, forming on average 2.9 H-bonds per water molecule. The remaining molecules in the 1 ML system are to be found further away from the sl interface (at $z \geq 0.139$ nm) and form three-dimensional clusters in which H-bonding also occurs between water molecules. The sharp peak occurring at $z = 0.139$ nm and $\theta_\mu = 180^\circ$ in Figure 3a indicates that these molecules orient their dipole moment vector toward the surface. Figure 6a illustrates a typical configuration ($t = 3.0$ ns) of the 1 ML system and summarizes the two observed H-bonding structures: the NW molecules are rendered as white and red spheres for H and O atoms, respectively, and the small number of molecules which also H-bond to other water molecules, forming three-dimensional clusters, which are rendered as green spheres. The results discussed above indicate that, at 1 ML coverage, the structure of water adsorbed on β -cristobalite is governed by W–Wall interactions.

3.2.2. $\delta = 2.2$ ML. A different orientational structure emerges on doubling the surface coverage to 2.2 ML, as illustrated in Figures 3b and 4b. To study the changes undergone by the orientational structure, we plot the θ_μ and θ_{OH} pdfs separately in Figure 7.

At $z = 0.039$ nm (Figure 7a,b, i.e., around the leading edge of $\rho(z)$ for $\delta = 2.2$ ML (cf. Figure 1a), water structure closely resembles that observed when $\delta = 1$ ML. This is shown by the maxima in the orientational pdfs (Figure 7a,b), found at $\theta_\mu \approx 110^\circ$ and $\theta_{OH} \approx 105^\circ$ (a secondary orientation is characterized by $\theta_{OH} \approx 0^\circ$ and $\theta_\mu \approx 60^\circ$), and confirmed by the H-bond connectivity information of panels b and c of Figure 1. The latter shows water forming <1 W–W H-bond and ~ 3 W–Wall

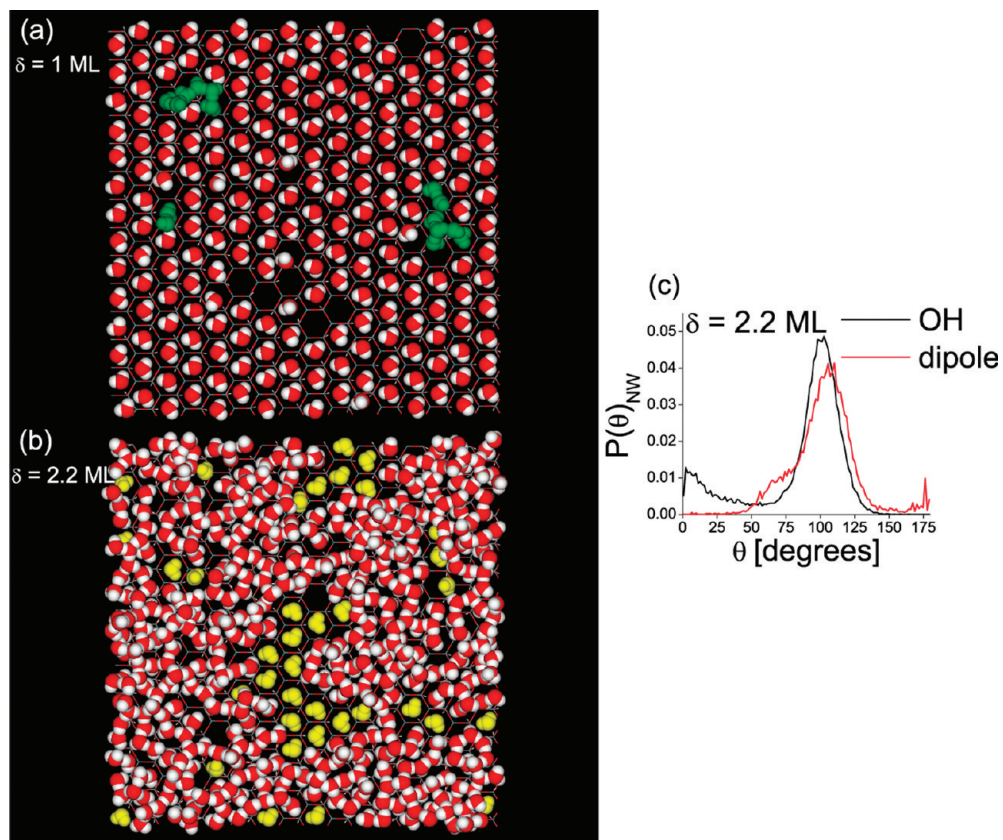


Figure 6. (a) Snapshot of the 1 ML system at $t = 3.0$ ns. Water molecules forming H-bonds with surface atoms only (“nonwetting”, NW), are rendered as red and white atoms, while those which also H-bond to other water molecules are shown in green. The underlying SiO₂ surface is shown as gray, red, and white lines. (b) Snapshot of the 2.2 ML system at $t = 3.0$ ns. NW water molecules are shown in yellow. Those which also form H-bonds with other water molecules are shown in red and white. (c) Angular probability density function for the NW molecules in (b).

H-bonds at $z = 0.039$ nm, indicating that water molecules in the first layer of the 2.2 ML film retain the NW properties observed when $\delta = 1$ ML. A representative configuration (collected at $t = 3.0$ ns) for the 2.2 ML system is given in Figure 6b, where the NW molecules are shown in yellow. We find that NW molecules represent $\sim 7\%$ of all molecules in the 2.2 ML system. In Figure 6c we present the orientational pdf's of the NW molecules shown in Figure 6b; the preferred orientation has both μ and OH approximately parallel to the surface, in agreement with the orientation of the predominantly nonwetting molecules at 1 ML coverage. The behavior of these NW molecules seems to be due to their inability to expose their OH vectors to water layers above them.⁴³

Further away from the surfaces, at $z = 0.089$ nm (coinciding with the maximum in $\rho(z)$), we observe three preferential orientations characterized by the dipole vector pointing into, parallel to, and away from, the surface ($\theta_\mu \approx 180^\circ$, 90° , and 0° , respectively; cf. Figure 7c). This contrasts with the single preferred orientation at $z = 0.089$ nm when $\delta = 1$ ML ($\theta_\mu \approx 110^\circ$ and $\theta_{OH} \approx 105^\circ$; cf. Figures 3a and 4a). The emergence of multiple orientational states in the 2.2 ML system can be attributed to W–W H-bond interactions, which occur rarely at 1 ML coverage. Their importance is confirmed in panels b and c of Figure 1 for $\delta = 2.2$ ML: at $z = 0.089$ nm, water molecules are involved in ~ 1.6 H-bonds with other water molecules and ~ 2 with the surface groups.

At a distance of $z = 0.139$ nm we find a larger number of possible orientational structures, as can be anticipated by the

broad peak in Figure 7e in the 90 – 120° range. Nonetheless, molecules have a tendency to orient their dipole vector into the surface, as denoted by the presence of peaks at $\theta_\mu \approx 180^\circ$ and $\theta_{OH} \approx 120^\circ$ in panels e and f of Figure 7. Finally, Figures 3b and 4b show the emergence of features characteristic of the lv interface near the smaller second peak in $\rho(z)$ ($z = 0.287$ nm).

The results shown above indicate that, for the majority of the molecules in the 2.2 ML system, W–W and W–Wall interactions are of comparable importance in determining liquid structure. Nonetheless, we find that the orientation of molecules immediately adjacent to the surface (representing $\sim 7\%$ of all water molecules), is determined predominantly by W–Wall H-bond interactions, as is the case when $\delta = 1$ ML.

3.2.3. $\delta = 4.3$ ML. The orientational structure in the 4.3-ML system is presented in Figure 8, where we show angular pdf's for selected positions along the film. At $z = 0.039$ nm (Figure 8a,b), water molecules orient both OH as well as μ forming angles of 110 – 120° with the surface normal; a second orientation in which one OH points away from the surface ($\theta_{OH} = 0^\circ$) is also possible. Most importantly, we note that this orientation arises from the formation of H-bonds with both surface groups (~ 3 per molecule) and other water molecules (~ 1 per molecule), as shown in Figure 1b,c.⁵³ The significant implication is that, unlike the molecules at $z = 0.039$ nm in thinner films ($\delta \leq 2.2$ ML), the 4.3 ML system shows no NW molecules.

It is important to reiterate that the occurrence of a W–W H-bond at $z = 0.039$ nm results in no alterations to the W–Wall H-bond connectivity, as previously observed in Figures 1b,c.

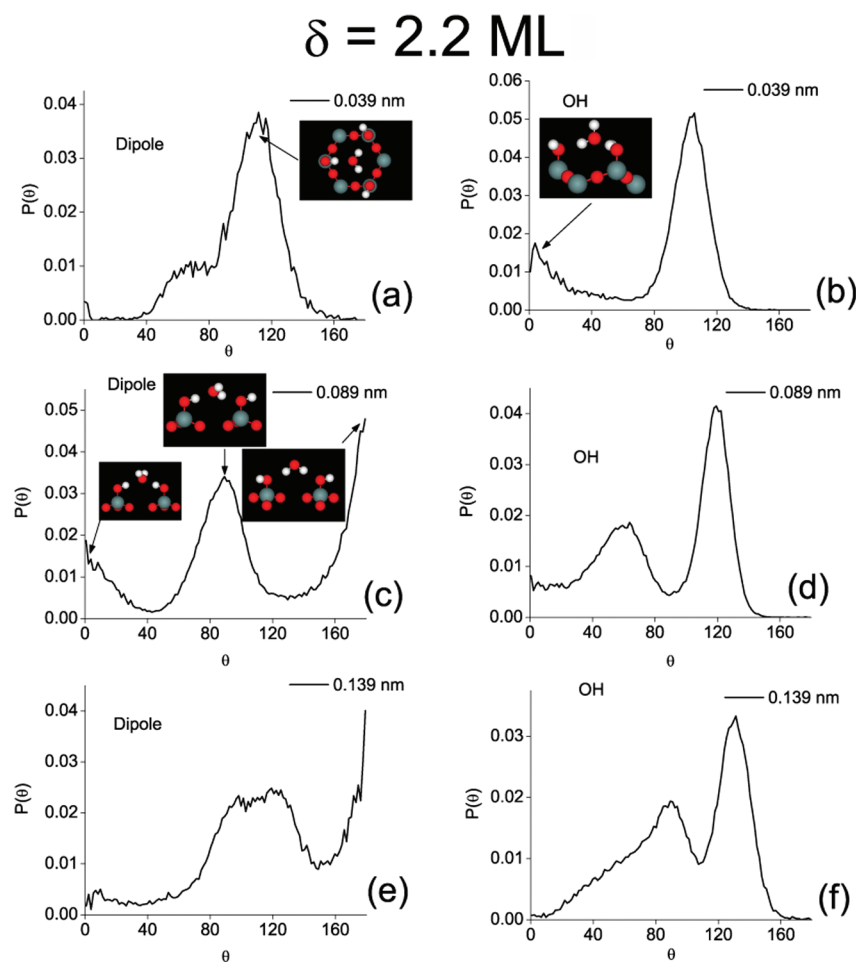


Figure 7. Orientational probability density functions, $P(\theta_\mu)$ (left column) and $P(\theta_{OH})$ (right column), in the 2.2 ML system for $z \leq 0.139$ nm (first peak in $\rho(z)$, Figure 1a). Insets to figures depict the orientation of water molecules relative to surface atoms in selected $P(\theta)$ peaks, through top (a) and lateral views (b, c).

Water molecules near the interface are therefore able to accommodate a W–W H-bond by tilting slightly the H–O–H molecular plane or by exposing an OH vector to the upper water layers. This is manifested by a $\sim 10^\circ$ increase in the value of the most probable θ_μ (relative to its value at $z = 0.039$ nm in the 2.2 ML system), and by the increase in peak height at $\theta_{OH} = 0^\circ$. Such a reorientation appears sufficient to accommodate a H-bond with water without compromising one of the 3 H-bonds with surface silanol groups.

Further away, at $z = 0.089$ and 0.139 nm (i.e., at and slightly beyond the first maximum in $\rho(z)$) the predominant water orientation is characterized by μ pointing into the surface (Figure 8c–f). The orientational structure at $z = 0.089$ nm results from the formation of ~ 2 H-bonds with surface silanol groups and the acceptance of ~ 1.7 H-bonds from water molecules present in layers further away from the surface (cf. Figure 1b,c). At $z = 0.089$ nm, the orientation of water contrasts with that observed at the same distance from the surface in the 2.2 ML system (shown in panels c and d of Figure 7); in the latter system, the dipole orientation can adopt three states of similar probability, while in the 4.3 ML system most molecules are found around $\theta_\mu = 180^\circ$. This orientation is due to H-bonding with water molecules located further away from the interface that “pin” those at $z = 0.089$ nm into a single preferential orientation.

The orientational structure becomes more diffuse at larger distances from the surface. However, we note two structural features at $z = 0.238$ nm and $z = 0.338$ nm, i.e., at the first local minimum and second maximum in $\rho(z)$, in Figure 1a. At the local minimum, panels g and h of Figure 8 show that molecules have a tendency to orient their dipole toward the surface, as shown by the peak at $\theta_\mu \approx 180^\circ$, while at the second maximum in $\rho(z)$, molecules have a tendency of orienting one of their OH groups into the surface. These orientational structures maximize the H-bonding of molecules at $z = 0.238$ and 0.338 nm—both participate ~ 3.5 W–W H-bonds—and that of molecules closer to the sl interface. As will be explained in the following section, the “OH-down” and “dipole-down” orientational structures appear alternatively in systems with larger values of δ .

3.2.4. $\delta = 15.1$ ML. We conclude this section discussing the orientational structure when $\delta = 15.1$ ML. Comparison of the orientational pdf's for $\delta = 4.3$ and 15.1 ML reveals a very similar orientational structure up to $z = 0.338$ nm. Figure 9 presents evidence of this observation, showing contour plots of $P(z, \theta)$ for $z \leq 0.4$ nm in 4.3 and 15.1 ML systems. Both sets of contour plots exhibit peaks at approximately the same positions on the (z, θ) plane. Thus, we conclude that the structure of water molecules nearest the sl interface ($z \leq 0.338$ nm) ceases to vary with δ once ~ 4 ML have been adsorbed on the surface. This observation is consistent with the data in Figures 1 and 2, which

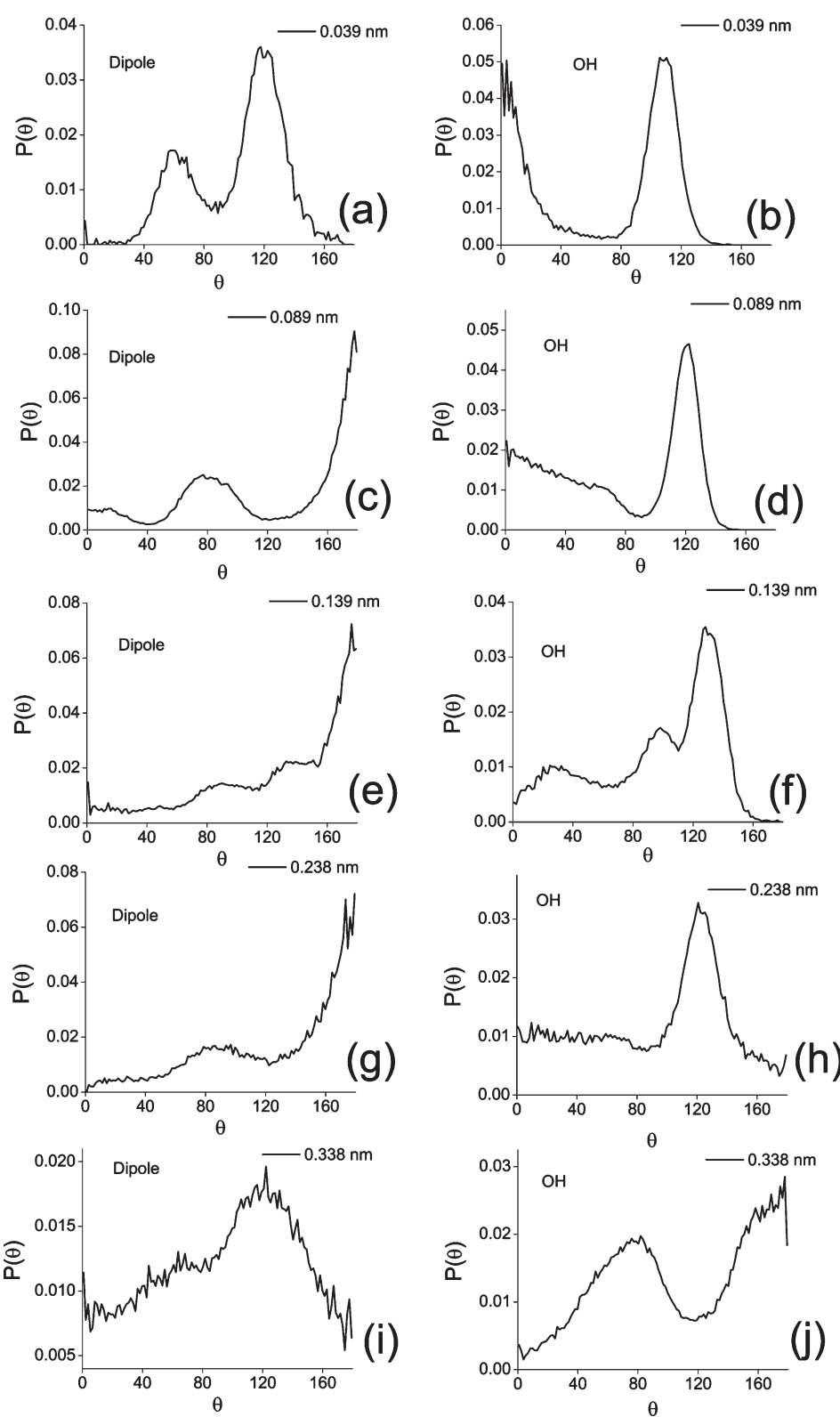
$\delta = 4.3 \text{ ML}$


Figure 8. Orientational probability density functions, $P(\theta_\mu)$ (left column) and $P(\theta_{OH})$ (right column), in the 4.3 ML system for selected peaks in $\rho(z)$ (Figure 1a). $z = 0.089, 0.238$, and 0.338 nm are the locations of the first maximum, first minimum, and second maximum of $\rho(z)$, respectively (cf. Figure 1a).

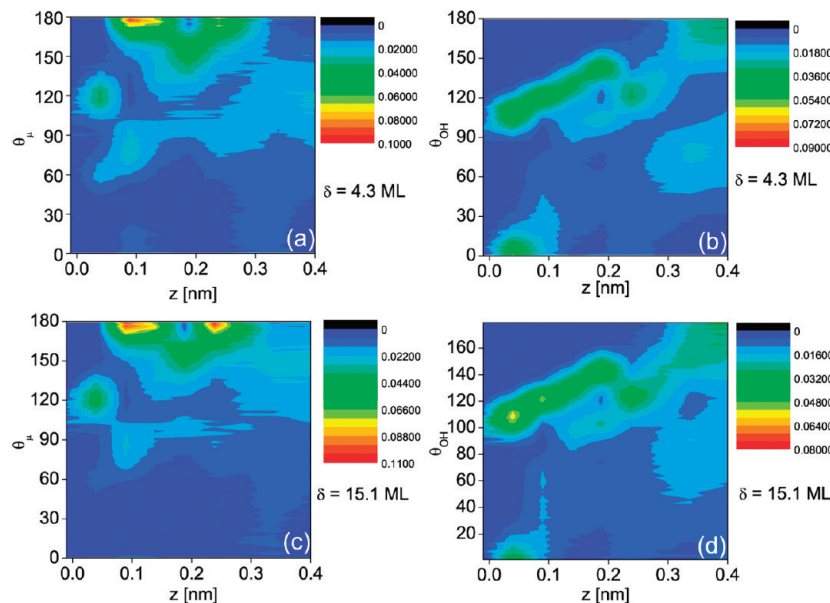


Figure 9. Contour plots describing the variation of $P(z, \theta_\mu)$ (left column) and $P(z, \theta_{OH})$ (right column) within 0.4 nm from the solid–liquid interface (present at $z = 0$) in thin films of thickness $\delta = 4.3$ ML (a, b) and 15.1 ML (c, d).

show that the density, H-bond, and potential energy profiles are similar for the two systems when $z \leq 0.338$ nm. At $z \geq 0.338$ nm we observe an orientational structure with a OH pointing into the surface, as in the 4.3 ML film at the same distance. Further away, a new orientational structure appears in the 15.1 ML film. This structure occurs at the same distance as the small peak in $\rho(z)$ (observed at $z = 0.536$ nm, cf. Figure 1a) and is characterized by μ pointing into the surface. From the above discussion, and that pertaining to the 4.3 ML film, it follows that molecules located near the $\rho(z)$ peaks of the 15.1 ML film switch their preferential orientation from “dipole-down” (i.e., μ pointing into the surface) at $z = 0.089$ nm (first $\rho(z)$ maximum), to “OH-down” (i.e., OH pointing into the surface) at $z = 0.338$ nm (i.e., the second maximum in $\rho(z)$), and back to “dipole-down” near the third small peak found at $z = 0.536$ nm.

4. SUMMARY AND CONCLUSIONS

The analysis presented in sections 3.1 and 3.2 reveals that, for the silica–water system investigated, film structural properties are determined by W–Wall interactions when $\delta \leq 1$ ML. At higher values of δ , W–W and W–Wall interactions are of comparable importance in determining the structure of water near the sl interface.

Predominance of W–Wall interactions when $\delta = 1$ ML is evident from the H-bonding connectivity, with water molecules forming 3 H-bonds with surface silanol groups and ~ 0 with other water molecules. This results in a single preferential orientation at the sl interface characterized by the μ and OH vectors being parallel to the surface.

The adsorption of water molecules beyond 1 ML coverage gives rise to W–W H-bond interactions that significantly modify the orientational structure at the sl interface. This can be appreciated in Figures 5, 7, and 8a–d, which show that water preferential orientations evolve from the single peak observed when $\delta = 1$ ML, to several peaks as film thickness increases. The onset of W–W interactions does not occur at the expense of W–Wall H-bonds, as can be observed in Figure 1c, where the

W–Wall H-bond connectivity is shown to be independent of δ . Therefore, as film thickness increases beyond 1 ML, water molecules at the sl interface that form 3 H-bonds with surface atoms are able to accommodate an additional H-bond from a nearby water molecule.

Water orientational structure near the sl interface evolves with δ up to a coverage of 4.3 ML. Beyond $\delta = 4.3$ ML, the orientational structure within 0.338 nm from the sl interface is independent of δ (cf. Figure 9). This suggests that water molecules at $z > 0.338$ nm do not influence the sl interfacial structure. When $\delta \geq 4.3$ ML, orientational order close to the surface ($z = 0.089$ nm, i.e., the first peak in $\rho(z)$) is characterized by molecules pointing their dipole vector into the surface, an orientation which favors the formation of 2 H-bonds with surface silanol groups plus 2 W–W H-bonds.^{15,14,54} Analysis of the orientational structure in the 15.1 ML film (Figures 3d and 4d) reveals that orientational correlations in the 15.1 ML film extend to distances up to ~ 1.4 nm from the sl interface, in agreement with experimental results,¹³ at which point a random, bulklike orientation is attained over a region that is roughly 0.2 nm in thickness, before the onset of the lv interface. Conversely, the other structural properties investigated ($\rho(z)$ and H-bonding) reach bulklike values at ~ 0.4 –0.6 nm from the sl interface.

To conclude, our study of thin film water adsorbed on β -cristobalite reveals the existence of a structural crossover concerning the relative influence of W–W and W–Wall interactions. In films up to 1 ML in thickness, structural properties are determined by W–Wall interactions, while results for films with more adsorbed layers suggest that W–W and W–Wall interactions are of comparable importance in determining structural properties such as H-bonding and molecular orientation. None of the films investigated revealed a scenario in which W–W H-bonds are formed at the expense of W–Wall interactions, indicating that, for proximal water, the latter remain as important as W–W interactions throughout the range of systems investigated.

A natural next step in the study of thin water films using simulations would involve the influence of substrate topography.

In particular, it would be interesting to study the effect of surface defects and impurities (such as the addition of hydrophobic moieties). In addition, an investigation into the structure of thin film water at room temperature would yield insights into the role of silica in the electrification of sandstorms.

AUTHOR INFORMATION

Corresponding Author

*E-mail: pdebene@princeton.edu.

ACKNOWLEDGMENT

I.A.A. gratefully acknowledges the financial support of the National Science Foundation (MRSEC DMR-0213706) and the Army Research Office (ARO-MURI W911NF-04-1-0170). P.G.D. gratefully acknowledges the financial support of the National Science Foundation (Collaborative Research in Chemistry Grant CHE-0908265). The authors thank Peter J. Rossky for useful comments on the manuscript.

REFERENCES

- (1) Thiel, P. A.; Madey, T. E. *Surf. Sci. Rep.* **1987**, *7* (6–8), 211–385.
- (2) Ewing, G. E. *Chem. Rev.* **2006**, *106* (4), 1511–1526.
- (3) Feibelman, P. J. *Phys. Today* **2010**, *63* (2), 34–39.
- (4) Hodgson, A.; Haq, S. *Surf. Sci. Rep.* **2009**, *64* (9), 381–451.
- (5) Verdaguer, A.; Sacha, G. M.; Bluhm, H.; Salmeron, M. *Chem. Rev.* **2006**, *106* (4), 1478–1510.
- (6) Iler, R. K. *The Chemistry of Silica*; John Wiley & Sons: New York, 1979.
- (7) Nangia, S.; Washton, N. M.; Mueller, K. T.; Kubicki, J. D.; Garrison, B. J. *J. Phys. Chem. C* **2007**, *111* (13), 5169–5177.
- (8) Yang, J. J.; Meng, S.; Xu, L. F.; Wang, E. G. *Phys. Rev. B* **2005**, *71* (3), No. 035413.
- (9) Yang, J. J.; Meng, S.; Xu, L. F.; Wang, E. G. *Phys. Rev. Lett.* **2004**, *92* (14), No. 146102.
- (10) Argyris, D.; Cole, D. R.; Striolo, A. *Langmuir* **2009**, *25* (14), 8025–8035.
- (11) Asay, D. B.; Kim, S. H. *J. Phys. Chem. B* **2005**, *109* (35), 16760–16763.
- (12) Barnette, A. L.; Asay, D. B.; Kim, S. H. *Phys. Chem. Chem. Phys.* **2008**, *10* (32), 4981–4986.
- (13) Verdaguer, A.; Weis, C.; Oncins, G.; Ketteler, G.; Bluhm, H.; Salmeron, M. *Langmuir* **2007**, *23* (19), 9699–9703.
- (14) Shen, Y. R.; Ostroverkhov, V. *Chem. Rev.* **2006**, *106* (4), 1140–1154.
- (15) Ostroverkhov, V.; Waychunas, G. A.; Shen, Y. R. *Phys. Rev. Lett.* **2005**, *94* (4), No. 046102.
- (16) Lu, Z. Y.; Sun, Z. Y.; Li, Z. S.; An, L. J. *J. Phys. Chem. B* **2005**, *109* (12), 5678–5683.
- (17) Berendsen, H. J. C.; Postma, J. P. M.; Vangunsteren, W. F.; Dinola, A.; Haak, J. R. *J. Chem. Phys.* **1984**, *81* (8), 3684–3690.
- (18) Berendsen, H. J. C.; Grigera, J. R.; Straatsma, T. P. *J. Phys. Chem.* **1987**, *91* (24), 6269–6271.
- (19) Lee, S. H.; Rossky, P. J. *J. Chem. Phys.* **1994**, *100* (4), 3334–3345.
- (20) Toukmaji, A. Y.; Board, J. A. *Comput. Phys. Commun.* **1996**, *95* (2–3), 73–92.
- (21) Ong, S. W.; Zhao, X. L.; Eisenthal, K. B. *Chem. Phys. Lett.* **1992**, *191* (3–4), 327–335.
- (22) Leung, K.; Nielsen, I. M. B.; Criscenti, L. J. *J. Am. Chem. Soc.* **2009**, *131* (51), 18358–18365.
- (23) Mahadevan, T. S.; Garofalini, S. H. *J. Phys. Chem. B* **2007**, *111* (30), 8919–8927.
- (24) Mahadevan, T. S.; Garofalini, S. H. *J. Phys. Chem. C* **2008**, *112* (5), 1507–1515.
- (25) Nicholson, D.; Parsonage, N. G. *Computer Simulation and the Statistical Mechanics of Adsorption*; Academic Press: London, 1982.
- (26) Puibasset, J.; Pellenq, R. J. M. *J. Chem. Phys.* **2003**, *119* (17), 9226–9232.
- (27) Puibasset, J.; Pellenq, R. J. M. *Phys. Chem. Chem. Phys.* **2004**, *6* (8), 1933–1937.
- (28) Rahaman, A.; Grassian, V. H.; Margulis, C. J. *J. Phys. Chem. C* **2008**, *112* (6), 2109–2115.
- (29) Stockelmann, E.; Hentschke, R. *Langmuir* **1999**, *15* (15), 5141–5149.
- (30) Castrillon, S. R. V.; Giovambattista, N.; Aksay, I. A.; Debenedetti, P. G. *J. Phys. Chem. B* **2009**, *113* (23), 7973–7976.
- (31) Starr, F. W.; Sciortino, F.; Stanley, H. E. *Phys. Rev. E* **1999**, *60* (6), 6757–6768.
- (32) Allen, M. P.; Tildesley, D. J. *Computer Simulation of Liquids*; Clarendon Press: Oxford, 1987.
- (33) Ryckaert, J. P.; Ciccotti, G.; Berendsen, H. J. C. *J. Comput. Phys.* **1977**, *23* (3), 327–341.
- (34) Giovambattista, N.; Debenedetti, P. G.; Rossky, P. J. *J. Phys. Chem. B* **2007**, *111* (32), 9581–9587.
- (35) Giovambattista, N.; Rossky, P. J.; Debenedetti, P. G. *Phys. Rev. E* **2006**, *73* (4), No. 041604.
- (36) Marti, J.; Padro, J. A.; Guardia, E. *J. Chem. Phys.* **1996**, *105* (2), 639–649.
- (37) Luzar, A.; Chandler, D. *Phys. Rev. Lett.* **1996**, *76* (6), 928–931.
- (38) Du, Q.; Freysz, E.; Shen, Y. R. *Science* **1994**, *264* (5160), 826–828.
- (39) Lee, C. Y.; Mccammon, J. A.; Rossky, P. J. *J. Chem. Phys.* **1984**, *80* (9), 4448–4455.
- (40) Wang, J. W.; Kalinichev, A. G.; Kirkpatrick, R. J.; Cygan, R. T. J. *Phys. Chem. B* **2005**, *109* (33), 15893–15905.
- (41) Bauer, B. A.; Warren, G. L.; Patel, S. *J. Chem. Theory Comput.* **2009**, *5* (2), 359–373.
- (42) Taylor, R. S.; Dang, L. X.; Garrett, B. C. *J. Phys. Chem.* **1996**, *100* (28), 11720–11725.
- (43) Salmeron, M.; Bluhm, H.; Tatarkhanov, N.; Ketteler, G.; Shimizu, T. K.; Mugarza, A.; Deng, X. Y.; Herranz, T.; Yamamoto, S.; Nilsson, A. *Faraday Discuss.* **2009**, *141*, 221–229.
- (44) Vega, C.; Abascal, J. L. F.; Conde, M. M.; Aragones, J. L. *Faraday Discuss.* **2009**, *141*, 251–276.
- (45) Xu, K.; Cao, P. G.; Heath, J. R. *Science* **2010**, *329* (5996), 1188–1191.
- (46) Stillinger, F. H. *Science* **1980**, *209* (4455), 451–457.
- (47) Stillinger, F. H.; Weber, T. A. *J. Phys. Chem.* **1983**, *87* (15), 2833–2840.
- (48) Wilson, M. A.; Pohorille, A.; Pratt, L. R. *J. Phys. Chem.* **1987**, *91* (19), 4873–4878.
- (49) The temperature at which our simulations were run is higher than the melting point of bulk SPC/E water (215 K⁴⁴). The presence of the silica substrate is likely to increase the melting temperature of water, though the extent to which thin film water is icelike remains an open question. Our simulations show evidence of mixed liquid-like/solid-like structural features, in agreement with experiments in refs ^{11–13} conducted at $T > T_{\text{melting}}$ (cf. section 3). Further, recent room-temperature AFM experiments⁴⁵ have also shown that the first two layers of water on mica, a hydrophilic substrate, have the structure of ice, whereas subsequent layers appear to be liquid-like.
- (50) Our estimate of the H-bond energy is also in agreement with the average H-bond energy computed from the total cohesive energy of water, -23 kJ mol^{-1} ⁴⁶, which accounts for small contributions to the binding energy arising from next-nearest and higher neighbors.
- (51) We compare the adsorption energy of the 1 ML system with that of the DFT study by Yang et al.⁸ The adsorption energy is defined as $E_{\text{ads}} = -(E_{\text{Total}} - E_{\text{Wall}} - NE_{\text{W}})/N$, where E_{Total} is the total potential energy of the system (including water and wall), E_{Wall} is the potential energy of the dry surface, and E_{W} is that of an isolated water molecule (set to zero). $E_{\text{ads}} > 0$ denotes binding. To compare our results with those of Yang et al.,⁸ we minimized the potential energy of an

equilibrium MD configuration, in order to obtain the inherent structure.⁴⁷ The value of E_{ads} at the (local) minimum is 76 kJ mol⁻¹ or ~ 790 meV. The DFT calculations⁸ arrived at $E_{\text{ads}} = 701$ meV for 1 ML and 768 meV for adsorption of a single water molecule. The difference in E_{ads} when $\delta = 1$ ML, relative to our work, can in part be attributed to the observation by Yang et al.⁸ of certain water molecules forming only two H-bonds with surface silanol groups. Our results show that >90% of molecules form three H-bonds with surface groups; this happens to be the structure predicted for single-molecule adsorption,⁸ and the agreement with our results is correspondingly better.

(S2) DFT calculations⁸ also found that certain water molecules form only two H-bonds with surface silanols (and zero with other water molecules). This second structure appears to agree with results from other classical MD simulations⁷ but was not found in our results.

(S3) The simulations of water confined between two SiO₂ surfaces by Lee and Rossky¹⁹ also showed surface water's involvement in three H-bonds with the surface O and H atoms, two as acceptor and one as donor. This configuration corresponds to the orientation in which one of the OH is parallel to the surface normal ($\theta_{\text{OH}} \approx 0^\circ$). As noted in parts a and b of Figure 8, we observe this orientational structure in addition to that in which μ and both OH are roughly parallel to the surface.

(S4) This orientational structure is consistent with that found for water at quartz interfaces using sum-frequency vibrational spectroscopy (SFVS).^{13,14} SFVS experiments over a broad range of pH conditions have provided evidence that water orients its H atoms toward the silica. A further orientation proposed by SFVS—not observed in our simulations—has the water O facing the surface.

(S5) It should be noted that water orientation at the lv interface depends on the form of the intermolecular potential, specifically on factors such as the quadrupole moment.⁴⁸ Results for the TIP4P model show that water orients its dipole vector roughly parallel to the lv interface.⁴⁸ This contrasts with the orientation observed in our work, and that of others using polarizable and nonpolarizable potentials,^{41,42} where it is found that water molecules tend to point their protons toward the vapor phase. We note that this model dependence is not an issue at the polar sl interface.